

# Modeling the segmentation clock as a network of coupled oscillations in the Notch, Wnt and FGF signaling pathways

Albert Goldbeter<sup>a,\*</sup>, Olivier Pourquié<sup>b,c</sup>

<sup>a</sup>*Faculté des Sciences, Université Libre de Bruxelles, Campus Plaine, C.P. 231, B-1050 Brussels, Belgium*

<sup>b</sup>*Howard Hughes Medical Institute, Kansas City, MO 64110, USA*

<sup>c</sup>*Stowers Institute for Medical Research, Kansas City, MO 64110, USA*

Received 26 November 2007; accepted 8 January 2008

Available online 18 January 2008

## Abstract

The formation of somites in the course of vertebrate segmentation is governed by an oscillator known as the segmentation clock, which is characterized by a period ranging from 30 min to a few hours depending on the organism. This oscillator permits the synchronized activation of segmentation genes in successive cohorts of cells in the presomitic mesoderm in response to a periodic signal emitted by the segmentation clock, thereby defining the future segments. Recent microarray experiments [Dequeant, M.L., Glynn, E., Gaudenz, K., Wahl, M., Chen, J., Mushegian, A., Pourquié, O., 2006. A complex oscillating network of signaling genes underlies the mouse segmentation clock. *Science* 314, 1595–1598] indicate that the Notch, Wnt and Fibroblast Growth Factor (FGF) signaling pathways are involved in the mechanism of the segmentation clock. By means of computational modeling, we investigate the conditions in which sustained oscillations occur in these three signaling pathways. First we show that negative feedback mediated by the Lunatic Fringe protein on intracellular Notch activation can give rise to periodic behavior in the Notch pathway. We then show that negative feedback exerted by Axin2 on the degradation of  $\beta$ -catenin through formation of the Axin2 destruction complex can produce oscillations in the Wnt pathway. Likewise, negative feedback on FGF signaling mediated by the phosphatase product of the gene *MKP3/Dusp6* can produce oscillatory gene expression in the FGF pathway. Coupling the Wnt, Notch and FGF oscillators through common intermediates can lead to synchronized oscillations in the three signaling pathways or to complex periodic behavior, depending on the relative periods of oscillations in the three pathways. The phase relationships between cycling genes in the three pathways depend on the nature of the coupling between the pathways and on their relative autonomous periods. The model provides a framework for analyzing the dynamics of the segmentation clock in terms of a network of oscillating modules involving the Wnt, Notch and FGF signaling pathways.

© 2008 Elsevier Ltd. All rights reserved.

**Keywords:** Model; Somitogenesis; Segmentation; Oscillation; FGF; Wnt; Notch

## 1. Introduction

The segmented or metamer aspect of the body axis is a basic characteristic of many animal species ranging from invertebrates to human. The vertebrate body is built on a metamer organization, which consists of a repetition along the antero-posterior (AP) axis of functionally equivalent units, each comprising a vertebra, its associated muscles, peripheral nerves and blood vessels. The segmented distribution of vertebrae derives from the earlier metamer pattern of the embryonic somites which are

epithelial spheres generated in a rhythmic fashion from the mesenchymal presomitic mesoderm (PSM). The segmental pattern was proposed to be established in the PSM by a mechanism involving an oscillator (the segmentation clock) which is thought to set the periodicity of the process (see scheme in Fig. 1), and a traveling wavefront defined by antagonistic gradients of the signaling molecules Fibroblast Growth Factor (FGF) and retinoic acid (RA), which controls the spacing mechanism of somite boundaries (Pourquié, 2003; Dubrulle and Pourquié, 2004; Delfini et al., 2005). We recently proposed a model in which the mutual antagonism of FGF and RA gradients generates a sharp threshold associated with a phenomenon of bistability (Goldbeter et al., 2007). This phenomenon, which

\*Corresponding author. Tel.: +32 2 650 5772; fax: +32 2 650 5767.

E-mail address: [agoldbet@ulb.ac.be](mailto:agoldbet@ulb.ac.be) (A. Goldbeter).

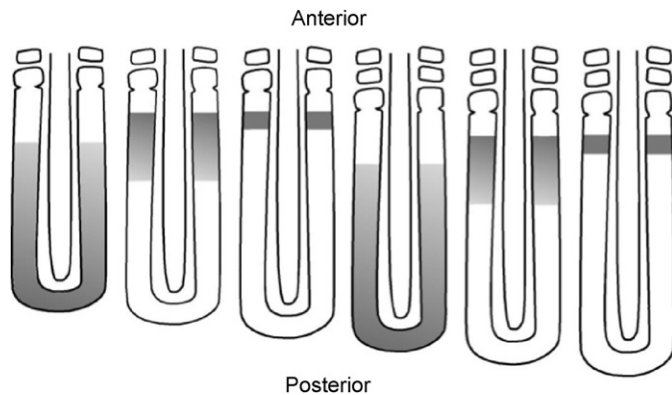


Fig. 1. Scheme illustrating the operation of the segmentation clock in the presomitic mesoderm (PSM) in chick embryos. Oscillations originate at the posterior end of the PSM and propagate as a transcription wave (in gray) toward the anterior end where the periodic signal emitted by the clock triggers the expression of genes, such as *Mesp2*, specific for somite formation (not shown). Each cycle of the segmentation clock oscillation corresponds to the formation of a new pair of somites. Growth of the PSM at the posterior end occurs continuously until the final number of somites is reached. The period of the segmentation clock in chick embryos is close to 90 min.

involves the coexistence between two stable steady states, is restricted to a defined AP level within the PSM. We suggested that the abrupt bistable steady-state switch that can occur in this window can explain the coordinated segmental gene activation which takes place in presumptive segments in response to the periodic signal of the segmentation clock.

The existence of the segmentation clock has been substantiated by numerous experimental observations, which first showed that genes in the Notch signaling pathway are expressed in a periodic manner, with a period of the order of 90 min in the chick embryo (Fig. 1) (Palmeirim et al., 1997; Pourquié, 2003; Giudicelli and Lewis, 2004). Negative feedback on gene expression appears to underlie the periodic transcription of the gene *Lunatic fringe* (*lfng*) (Dale et al., 2003). The segmentation clock also involves oscillations in the Wnt signaling pathway, which appear to govern the periodic operation of the Notch pathway (Aulehla et al., 2003). Microarray studies of the mouse PSM transcriptome recently revealed (Dequeant et al., 2006) that the oscillator associated with the segmentation clock drives the periodic expression of a large network of cyclic genes involved in the Notch, Wnt and also the FGF signaling pathways. The cyclic genes identified in the Notch and FGF pathways oscillate synchronously, but in antiphase with respect to the cyclic genes in the Wnt pathway. By this microarray approach, six of the eight known mouse cyclic genes—*Hes1*, *Hes5*, *Hey1*, *Lfng*, *Axin2* and *Nkd1*—were identified with periods of 94, 102, 112, 81, 102 and 112 min, respectively (Dequeant et al., 2006). The observations of Dequeant et al. (2006) throw light on the molecular nature of the segmentation clock and suggest that it relies on coupled

oscillations in the Wnt, FGF and Notch signaling pathways. The antiphase relationship between the genes cyclically expressed in the FGF and Notch pathways on one hand, and the Wnt pathway on the other hand, further points to the existence of cross-talk between the FGF/Notch and Wnt pathways possibly in the form of mutual inhibition (Dequeant et al., 2006).

Here, turning to the nature of the oscillatory process involved in the clock and wavefront mechanism (Cooke and Zeeman, 1976), we propose a model for the segmentation clock in amniotes like chick and mouse. The model is based on a network of coupled oscillators in the Wnt, FGF and Notch signaling pathways. We first show how oscillations can occur in each of the three pathways, as a result of negative feedback regulation, in the presence of a constant level of an external triggering signal. We then study the oscillatory behavior of the coupled Notch–Wnt–FGF signaling network and discuss possible mechanisms capable of accounting for the tight temporal coordination of cycling genes oscillations in the mouse PSM. Our approach at this stage is qualitative rather than quantitative, as we wish to explore the dynamical consequences of negative feedback regulation within each pathway and of the coupling between the Wnt, Notch and FGF pathways without trying to use experimentally established parameter values, many of which have yet to be determined. By including the interactions between the FGF, Wnt and Notch signaling pathways the model differs from previously proposed models which show how autonomous oscillations can arise due to Notch signaling in zebrafish (Lewis, 2003; Monk, 2003) or to the interaction between Notch and Wnt signaling in mice (Rodriguez-Gonzalez et al., 2007).

The modeling approach allows us to address a series of questions: (i) can the coupling of the Notch, Wnt and FGF oscillators result in their synchronization? (ii) Does synchronization require that the autonomous periods of the three oscillating pathways, i.e. their period in the absence of coupling, be sufficiently close to each other? (iii) Can quasiperiodic, complex periodic or aperiodic (i.e. chaotic) oscillations result from the coupling of the three oscillating pathways when their autonomous periods are too far apart from each other? (iv) Is mutual inhibition required to explain the antiphase oscillations in the Wnt and in the FGF/Notch pathways, or can this phase relationship be obtained in other conditions?

Together with Marc Kirschner and co-workers, Reinhart Heinrich modeled in great detail signal transduction in the Wnt signaling pathway (Lee et al., 2003; Krüger and Heinrich, 2004), without focusing, however, on the possibility of oscillatory behavior. Here we examine the conditions in which oscillations in the segmentation clock might arise in the Wnt pathway, and also in the Notch and FGF pathways, as a result of negative feedback regulation. The model supports the view (Dequeant et al., 2006) that the network formed by these three signaling pathways

functioning as coupled oscillators underlies the segmentation clock that controls somitogenesis.

## 2. Oscillations in the Notch pathway

The possibility that the segmentation clock involves oscillations in the Notch signaling pathway was the first documented experimentally (Palmeirim et al., 1997; Dale et al., 2003) and was previously considered theoretically by Lewis (2003) in zebrafish and Monk (2003) in mouse, on the basis of negative feedback involving the *Hairy*-related genes. This family of transcription factors codes for negative regulators that are able to regulate their own transcription and in some cases act downstream of Notch. Oscillations of the mouse *Hairy* and enhancer of split genes *Hes7* and *Hes1* were reported in the mouse PSM, and *Hes1* oscillations were also observed in fibroblast cell cultures synchronized by a serum shock (Hirata et al., 2002). These authors also showed that *Hes7* negatively regulates its own transcription as well as that of *Lunatic Fringe* (Bessho et al., 2003) and *Hes1* and *Hes7* oscillations could be modeled in terms of negative feedback (Hirata et al., 2002, 2004). Oscillations of the *Hairy*-related genes have been considered to reflect periodic Notch activation, but recent experiments in zebrafish argue against a role of this pathway in the control of *Her* genes oscillations. These results suggest that Notch is not required for *Her* oscillations and that the major role of Notch in the system is to synchronize the oscillatory behavior between cells (Jiang et al., 2000; Riedel-Kruse et al., 2007). In amniotes like mouse and chick, however, Notch signaling is required for the oscillations of cyclic genes such as *Lunatic fringe*. Furthermore, Notch-dependent negative feedback circuits involving genes such as *Lunatic fringe*, which acts by inhibiting the Notch pathway, have been described in

mouse and chick (Dale et al., 2003; Morimoto et al., 2005). Oscillatory *Lunatic fringe* expression appears to play a key role in somitogenesis (Serth et al., 2003).

Here we focus on a model of the Notch module of intermediate complexity, which is schematized in Fig. 2c. The Delta ligand binds to the Notch cell surface receptor, activating its enzymatic cleavage at the membrane level, which releases the Notch intracellular domain (NICD) in the cytoplasm. The latter migrates to the nucleus where it induces the expression of genes such as *Lunatic fringe*. The protein product of the latter gene, Lunatic Fringe, inhibits the cleavage of Notch into NICD, thus creating a negative feedback loop in Notch signaling. Here we do not consider explicitly the *Hes7* based negative feedback loop because its relationship with the Notch pathway is still unclear.

The temporal evolution of the Notch module is governed by the kinetic equations Eqs. (A.1)–(A.5) given in Appendix A. This set of ordinary differential equations describes the time evolution of the five variables of the Notch module, which are the concentrations of: Notch, NICD, nuclear NICD, mRNA of the *Lunatic fringe* gene and Lunatic Fringe protein. For an appropriate set of parameter values, numerical integration of the kinetic equations Eqs. (A.1)–(A.5) shows that sustained oscillations in all five variables can occur in a given range of (constant) Notch levels. The *Lunatic fringe* gene is expressed periodically (see the oscillatory time course of its mRNA in Fig. 3), as a result of oscillations in the level of the active form of the transcriptional regulator, NICD. Here the negative feedback is not exerted directly at the transcriptional level, but rather at an early step of activation of the transcriptional regulator NICD preceding its translocation into the nucleus. This is in contrast to the negative feedback on transcription that plays a key role in

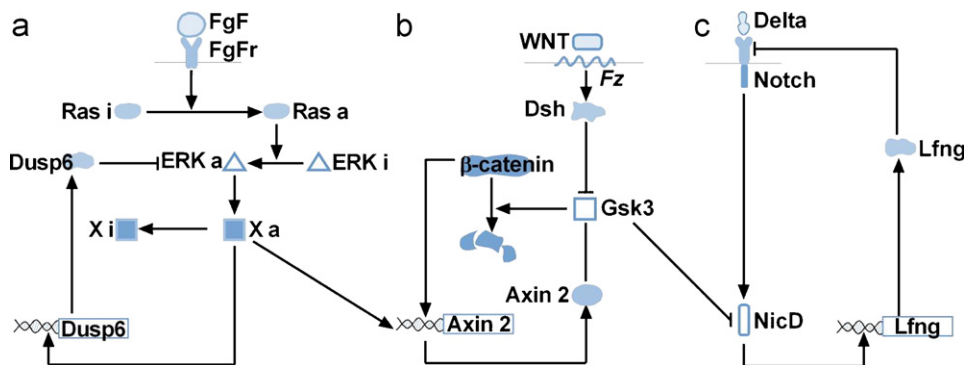


Fig. 2. Model for the segmentation clock based on negative feedback loops in the coupled FGF, Wnt and Notch signaling pathways. The negative feedback in the FGF module (a) is based on the inhibition exerted on FGF signaling by the phosphatase Dusp6 that is induced in the FGF signaling pathway. The negative feedback in the Wnt module (b) is based on the induction of Axin2 accumulation by  $\beta$ -catenin and the participation of Axin2 in the destruction complex, consisting of Axin2 and kinase Gsk3, which leads to  $\beta$ -catenin degradation. The negative feedback in the Notch module (c) involves the inhibition exerted by the protein Lunatic Fringe, induced by Notch signaling, on Notch activation into its intracellular domain NICD. These negative feedback loops can produce autonomous, sustained oscillations in each of the three signaling modules (Fig. 3). When the three modules are coupled, they cease to oscillate at their own, distinct period and become synchronized if their periods prior to coupling are sufficiently close to each other (Fig. 4). Two coupling interactions are shown, for illustrative purpose. First, free Gsk3 inhibits the activation by NICD of *Lunatic fringe* gene expression, which couples Wnt to Notch signaling. Second, the transcription factor  $X_a$  activated in the FGF signaling pathway co-induces the expression of the *Axin2* gene, together with  $\beta$ -catenin. This regulation couples FGF to Wnt signaling (see text for further details).

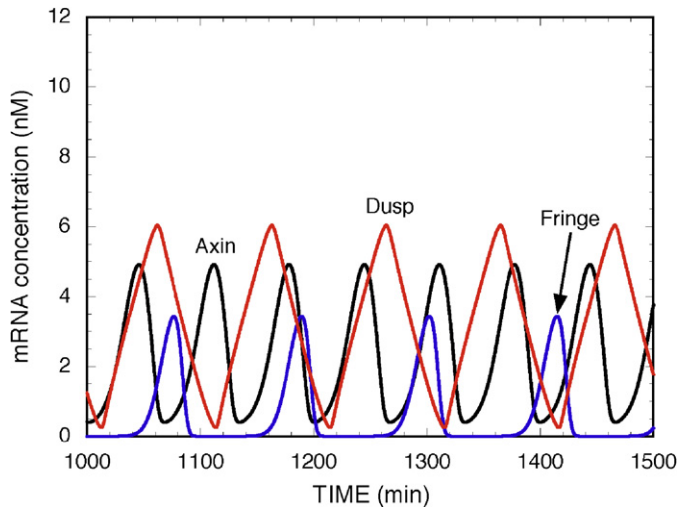


Fig. 3. Oscillations in the Notch, Wnt and FGF modules in the absence of coupling between the three signaling pathways. The curves show the oscillatory mRNA profiles corresponding to periodic expression of the genes *Lunatic fringe* in the Notch pathway, *Axin2* in the Wnt pathway, and *MKP3/Dusp6* in the FGF pathway. The data were obtained by numerical integration of Eqs. (A.1)–(A.16) which govern the time evolution of the Notch, Wnt and FGF modules, respectively (see Appendix). Numerical integration was performed by means of the Berkeley Madonna program, using the routine for stiff differential equations. Because the three pathways are uncoupled, each oscillates with a distinct autonomous period. Consequently, in contrast to what occurs in the case of coupling (see Fig. 4), the phase relationship between the genes oscillating in the three pathways changes in the course of time. Parameter values selected for the three modules (see Table A.1 in Appendix) give a period close to 66, 100 and 113 min for the mRNAs of *Axin2*, *MKP3/Dusp6* and *Lunatic fringe*, respectively.

the molecular mechanism of circadian rhythms (Dunlap, 1999; Goldbeter, 2002).

### 3. Oscillations in the Wnt pathway

Turning to the Wnt signaling module, we consider the minimal model schematized in Fig. 2b. The Wnt signal triggers the synthesis of the protein Dishevelled (Dsh) which inhibits the protein kinase Gsk3 in a Dsh-dependent manner. Gsk3 then forms with the protein Axin2 and with  $\beta$ -catenin the “destruction complex”, which phosphorylates  $\beta$ -catenin into the form  $\beta$ -catenin-P marked for degradation by the proteasome machinery. Inhibition of Gsk3 by Dsh results in inhibition of the destruction complex and allows the accumulation of  $\beta$ -catenin, which then migrates to the nucleus and triggers the expression of a number of genes, among which the gene of Axin2. The ensuing synthesis of the Axin2 protein contributes to increase the level of the destruction complex, thereby inducing a decrease in the level of  $\beta$ -catenin. This negative feedback loop differs in nature from that described above for the Notch signaling module. Here, negative feedback operates via the formation of a protein complex allowing the destruction of the transcription factor  $\beta$ -catenin that

leads to the accumulation of a protein, Axin2, involved in the very formation of this destruction complex.

The temporal evolution of the Wnt module is governed by the kinetic equations Eqs. (A.6)–(A.11) given in Appendix A. This set of ordinary differential equations describes the time evolution of the six variables of the Wnt module, which are the concentrations of: the kinase Gsk3, the cytosolic dephosphorylated and phosphorylated forms of  $\beta$ -catenin, the nuclear form of  $\beta$ -catenin, the Axin2 mRNA, and the Axin2 protein. In simulating the effect of the Wnt signal, we do not consider Wnt explicitly but assume that a constant level of Wnt corresponds to a constant level of Dsh, which is treated as a parameter.

Here again, for an appropriate set of parameter values, numerical integration of the kinetic equations Eqs. (A.6)–(A.11) shows that sustained oscillations in all six variables can occur in a given range of (constant) Wnt levels. The Axin2 and Gsk3 proteins oscillate out of phase. Representative of the oscillating dynamics of the Wnt pathway, the periodic variation of Axin2 mRNA is shown in Fig. 3. The period of the oscillations in Axin2 mRNA can differ from that of oscillations of *Lunatic Fringe* mRNA in the Notch pathway shown in Fig. 3, since the two signaling pathways are not coupled at this stage and therefore function as independent oscillators.

### 4. Oscillations in the FGF pathway

The highly simplified model for the FGF signaling module is represented schematically in Fig. 2a. We consider that the FGF signal triggers the activation of Ras, which eventually activates the MAP kinase ERK into ERK<sub>a</sub>. The latter kinase, through reversible phosphorylation, activates a transcription factor, denoted X, which probably belongs to the ETS family (Lunn et al., 2007). This transcription factor induces the expression of the gene *MKP3/Dusp6*, which encodes a phosphatase that inactivates ERK<sub>a</sub> (Li et al., 2007) (similar results are obtained when assuming that the phosphatase MKP3/Dusp6 inactivates the active, phosphorylated form of Ras). The resulting negative feedback loop differs in nature from those described above for the Notch and Wnt signaling modules. Here, negative feedback is based on inactivation of a component of the FGF signaling pathway through dephosphorylation by a phosphatase induced by FGF signaling. Because the regulation is based on reversible protein phosphorylation, we assume that the total amounts of ERK and X remain constant so that the proteins alternate periodically between their active and inactive forms in the course of FGF-triggered oscillations.

The temporal evolution of the FGF module is governed by the kinetic equations Eqs. (A.12)–(A.16) given in Appendix A. This set of ordinary differential equations describes the time evolution of the five variables of the FGF module, which are the concentrations of: the active forms of Ras, ERK and of the transcription factor X, *MKP3-Dusp6* mRNA, and the phosphatase MKP3-Dusp6.

Numerical integration of the kinetic equations Eqs. (A.12)–(A.16) shows that for an appropriate set of parameter values, sustained oscillations in all five variables can occur in a given range of (constant) FGF levels. We illustrate the oscillatory dynamics of the FGF pathway by showing in Fig. 3 the periodic evolution of *MKP3-Dusp6* mRNA. We note again that the period of oscillations in *MKP3-Dusp6* mRNA can differ from that of oscillations of *Lunatic fringe* mRNA in the Notch pathway and of *Axin2* mRNA in the Wnt pathway, since the three signaling modules are not coupled at this stage and therefore oscillate in parallel at their own pace.

### 5. Coupling oscillations in the Notch, Wnt and FGF signaling pathways

Several observations indicate that oscillations in the Notch, Wnt and FGF pathways can occur independently from each other, i.e. in parallel, but are nevertheless coupled in physiological conditions. Moreover, a hierarchy appears to exist, as Wnt oscillations drive oscillations in the Notch pathway (Aulehla et al., 2003). FGF appears to act upstream of Wnt, which acts upstream of Notch (Niwa et al., 2007; Wahl et al., 2007). Oscillations in the FGF pathway can occur in the absence of Notch signaling (Dequeant et al., 2006). Finally, the mouse transcriptome study shows that cycling genes in the Notch and FGF pathways oscillate synchronously, in antiphase with cycling genes from the Wnt pathway. These observations suggest that the Wnt pathway may be coupled to the FGF and Notch pathways through mutual inhibition (Dequeant et al., 2006). The precise nature of such a coupling remains unclear, but mutual inhibition of the FGF and Wnt pathways has been reported in other developmental processes such as sex determination in mammals (Kim et al., 2006). In the absence of precise information about the nature of cross-talk between Wnt, Notch and FGF signaling in the course of somitogenesis in the PSM, we will examine one hypothetical mode of coupling between these signaling pathways to show that it can readily lead to synchronization of the three oscillating modules.

For coupling the Wnt and Notch pathways we will assume, for simplicity, that the free form of the kinase Gsk3 (K), which plays a key role in the Wnt pathway (see Fig. 2), directly inhibits the activation of *Lunatic fringe* expression by the nuclear form of NICD in the Notch pathway. This assumption is one way to express the observation that Gsk3 can exert a negative regulation on Notch signaling (Espinosa et al., 2003). Then the maximum rate  $v_{sF}$  of expression of the *Lunatic fringe* gene in Eq. (A.4) is replaced by the rate  $v_{sFK}$  given by Eq. (A.17). For coupling the Wnt and FGF pathways, we assume that the expression of the gene *Axin2* in the Wnt pathway is induced not only by  $\beta$ -catenin but also by the transcription factor X activated in the FGF pathway. The kinetic Eq. (A.10) governing *Axin2* gene expression must then be replaced by Eq. (A.18). This is one way of reflecting

the fact that FGF acts upstream of Wnt (Wahl et al., 2007).

In coupling the Wnt, Notch and FGF signaling pathways we therefore assume a direct inhibitory effect of the Wnt pathway on the Notch pathway through the kinase Gsk3, as well as a direct activating effect of the FGF pathway on the Wnt pathway through induction by transcription factor X of *Axin2* expression. Let us stress again that these particular modes of coupling are retained here for illustrative purpose mainly. Many other types of coupling are possible, some of which involve mutual activation or inhibition. The assumptions retained here hold with the observations that Wnt acts upstream of Notch and that FGF acts upstream of Wnt.

When the dynamics of the coupled system formed by the Wnt, Notch and FGF modules is determined by numerical integration of Eqs. (A.1)–(A.16) subjected to the changes specified by Eqs. (A.17) and (A.18), sustained oscillations are again obtained, but in contrast to the case of independent oscillations when the three signaling pathways are uncoupled and oscillate each at their own pace (Fig. 3), the oscillations in the Wnt, Notch and FGF pathways are now synchronized (Fig. 4). In the presence of coupling, the oscillations in the concentrations of mRNAs of *Lunatic fringe*, *Axin2* and *MKP3-Dusp6* have indeed the same

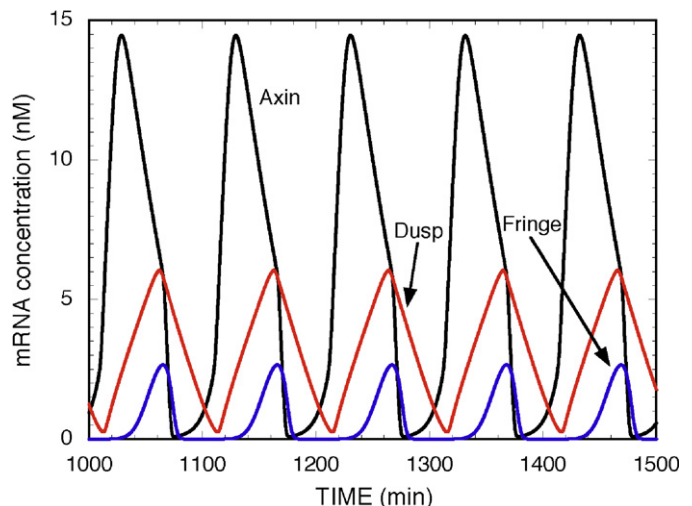


Fig. 4. Synchronized oscillations in the Notch, Wnt and FGF modules in the presence of coupling between the three signaling pathways. As in Fig. 3, the curves show the oscillatory mRNA profiles corresponding to periodic expression of the genes *Lunatic fringe* in the Notch pathway, *Axin2* in the Wnt pathway, and *MKP3/Dusp6* in the FGF pathway. The data are obtained by numerical integration of Eqs. (A.1)–(A.16) governing the time evolution of the Notch, Wnt and FGF modules, respectively (see Appendix A), subjected to the changes expressed by Eqs. (A.17) and (A.18). Numerical integration was performed by means of the Berkeley Madonna program, using the routine for stiff differential equations. Parameter values are the same as in Fig. 3, and are listed in Table A.1; the values of the additional parameters appearing in Eqs. (A.17) and (A.18) are also listed in Table A.1. Because the three pathways are now coupled, each oscillates with the same period, close to 100 min, and the phase relationships between the genes oscillating in the three pathways remain fixed in the course of time.

period and possess fixed phase relationships with respect to each other. As observed in the experiments (Dequeant et al., 2006), the *Lunatic fringe* and *MKP3-Dusp6* genes are expressed well out of phase with respect to the *Axin2* gene in the Wnt pathway, even though the oscillations are not fully in antiphase.

The amplitude of *Axin2* mRNA oscillations is higher than in the case of Fig. 3. This is due to our assumption that in the case of coupling, transcription of the *Axin2* gene is induced not only by  $\beta$ -catenin but also by the transcription factor X activated in the FGF signaling pathway. Because the same rate of induction by  $\beta$ -catenin is used in the two cases, the additional induction by X enhances the synthesis of *Axin2* mRNA.

When oscillations in the Wnt, Notch and FGF signaling pathways synchronize, their phase relationships closely depend on the nature of the cross-talk between the three pathways. Also influencing the phase relationships are the relative values of the autonomous period of each of the three oscillating pathways prior to coupling. The kinetic equations for the FGF, Wnt and Notch signaling modules were multiplied by scaling parameters  $\eta$ ,  $\varepsilon$ , and  $\theta$  (see Appendix A) so that the relative periods of the three oscillators could easily be changed.

## 6. Discussion

The segmentation clock that controls the periodic formation of somites in vertebrate embryos provides one of the most remarkable examples of biological rhythm. This oscillatory phenomenon plays a key physiological role in embryogenesis, and is characterized by the fact that it combines temporal with spatial self-organization (Pourquié, 2003). The existence of a segmentation clock was initially hypothesized on theoretical grounds (Cooke and Zeeman, 1976). Experimental evidence for its existence was first obtained in the form of periodic expression of genes associated to the Notch pathway (Palmeirim et al., 1997; Dale et al., 2003), and to the Wnt pathway (Aulehla et al., 2003). Recent microarray experiments on the mouse embryonic transcriptome confirmed that gene expression in the Wnt and Notch signaling pathways oscillates with the period of the segmentation clock, and further showed that genes of the FGF signaling pathway oscillate in phase with those of the Notch pathway, and in antiphase with periodic transcriptional activity in the Wnt pathway (Dequeant et al., 2006).

In this paper, we examined by means of computational modeling the view (Dequeant et al., 2006) that the Wnt, Notch and FGF signaling pathways oscillate as a result of negative feedback regulation and synchronize to form a network of periodically expressed genes that underlies the segmentation clock. We considered a model of intermediate complexity for each of the Wnt, Notch and FGF modules and showed that sustained oscillations can indeed occur in each of these pathways in an autonomous manner, i.e. in the absence of coupling between the three signaling

pathways. The nature of the negative feedback loop that is responsible for oscillatory behavior differs in each case. In the Notch pathway, the Lunatic Fringe protein induced by Notch signaling inhibits the enzymatic cleavage of the Notch ligand into its active intracellular moiety NICD. In Wnt signaling, it is the protein Axin2 induced by  $\beta$ -catenin upon Wnt stimulation that forms with the kinase Gsk3 the destruction complex that leads to  $\beta$ -catenin degradation. Finally, in the FGF pathway, the phosphatase MKP3-Dusp6 induced by FGF signaling inhibits, through dephosphorylation, a preceding step in the FGF signal transduction cascade.

In view of the disparity of these regulatory mechanisms, there is no reason that autonomous oscillations in the three signaling pathways should be characterized by the same, unique period. This is the reason why in the absence of coupling, the oscillations shown in Fig. 3 occur with different periods for the expression of the *Lunatic fringe* gene in the Notch pathway, the *Axin2* gene in the Wnt pathway and the gene *MKP3/Dusp6* in the FGF pathway. We nevertheless chose, arbitrarily, parameter values such that the three periods differ but remain sufficiently close to each other. Thus, in the case considered, the mRNAs of *Axin2*, *Lunatic fringe* and *MKP3/Dusp6* oscillate with a period close to 66, 113 and 100 min, respectively. This situation allows for the synchronization of the three signaling pathways when coupling between them is introduced (Fig. 4). The period of the synchronized oscillations is then equal to the period of the FGF oscillator, i.e. 100 min. Dominance by this module results from the hierarchy of regulations considered between the three oscillatory signaling pathways. If synchronization of the three pathways is needed for proper operation of the segmentation clock, we may expect that values of the biochemical parameters for each pathway were selected in the course of evolution so as to produce periods sufficiently close to one another.

Experimental observations indicate that cycling genes in the Notch pathway oscillate in phase with those in the FGF pathway, but in antiphase with cycling genes in the Wnt pathway (Dequeant et al., 2006). The present results show that such phase relationships might not necessarily be indicative of direct mutual inhibition between the Wnt pathway, and the FGF and Notch pathways. Here, we obtained oscillations of *Axin2* mRNA well out of phase with respect to those of *Dusp6* and *Lunatic fringe* mRNAs by assuming that FGF signaling activates *Axin2* expression in the Wnt pathway, while Gsk3 in the Wnt pathway inhibits *Lunatic fringe* expression in the Notch pathway (see Fig. 2). Such regulatory interactions do not appear to reduce simply to mutual inhibition between Wnt with respect to Notch and FGF signaling. The antiphase relationship observed in the experiments could thus also depend on the relative periods of the oscillators prior to coupling and might thus originate, in principle, from a variety of interactions between the three signaling pathways.

Synchronization of the Wnt, Notch and FGF pathways requires that the autonomous periods of the three modules in the absence of coupling do not differ too much from each other. Complex oscillatory phenomena can occur in the absence of synchronization. We expect that aperiodic oscillations corresponding to autonomous chaos or even multiple coexisting oscillatory regimes might also arise in such conditions, as observed in a variety of models in which multiple oscillatory mechanisms are coupled within the same biochemical system (Goldbeter, 1996). In the coupled model, we observed complex periodic oscillations or quasiperiodic oscillations. We also observed subharmonic entrainment, for example when the Wnt and Notch oscillators have a much shorter period than the FGF oscillator. Several rounds of gene expression in the Wnt and/or Notch modules can then occur for one round of gene expression in the FGF pathway. More detailed studies of the model for the coupled Wnt, Notch and FGF pathways should allow us to further clarify the conditions in which synchronization occurs between the three signaling modules.

The precise nature of the coupling between the Wnt, Notch and FGF modules remains to be clarified at the molecular level. Many interactions have been reported (Ishikawa et al., 2004), via direct mutual inhibition of Wnt and FGF signaling as in mammalian sex determination (Kim et al., 2006), or via the involvement of Gsk3 in both the Wnt and Notch signaling pathways (Espinosa et al., 2003). Direct activation of Notch signaling by Wnt has been reported (Hofmann et al., 2004; Galceran et al., 2004). Other modes of coupling between the three signaling pathways are possible. Thus, the protein *Sprouty*, an inhibitor of the FGF pathway, is induced by  $\beta$ -catenin, which would create a coupling between the Wnt and FGF modules (Katoh and Katoh, 2006). Here we considered two hypothetical examples of cross-talk between the three pathways to explore the consequences of coupling between oscillations in the Wnt, Notch and FGF modules. The interactions between the three pathways are likely to be more numerous and varied than those considered here.

We did not perform a detailed numerical analysis to determine the domains of sustained autonomous oscillations in parameter space for each of the three signaling modules. Clearly oscillations occur only in precise conditions, often in a range bounded by two critical values of a control parameter. To obtain synchronized oscillations between the FGF, Wnt and Notch pathways, it is not necessary that oscillations occur in all three signaling modules in the absence of coupling. Autonomous oscillations in one or two of these pathways could suffice to entrain the remaining, non-oscillatory module(s). This aspect deserves to be explored further and compared with the results of experimental studies in which one of the pathways is modified (Niwa et al., 2007; Wahl et al., 2007).

The model outlined here should also allow us to couple the segmentation clock with the mechanism that governs developmental transitions at the determination front level in the PSM. We recently showed by means of a theoretical model that the antagonistic gradients of RA and FGF along the PSM are capable of producing a bistability phenomenon involving sharp transitions between two stable steady states, as a result of mutual inhibition of RA and FGF signaling (Goldbeter et al., 2007). It is conceivable that the periodic signal from the segmentation clock drives the transition of a group of cells—which later will be committed to form a somite—from a state of high FGF, low RA to a state of low FGF, high RA. The question arises as to how the segmentation clock might impinge on FGF and/or RA signaling to trigger this bistable transition? One way is by activation of RA synthesis by Wnt signaling, through induction of the gene *Raldh2*, which encodes the Ra-synthesizing enzyme (Olivera-Martinez and Storey, 2007). Based on the observations of Dequeant et al. (2006) showing that the FGF pathway can oscillate much as the Wnt and Notch pathway, the present results raise an alternative possibility. Perhaps the role of bistability is to allow oscillations on the upper branch (high FGF) and to prevent them on the lower branch (low FGF, high RA), thus allowing cell differentiation when the level of FGF is constant and low instead of oscillating (with Notch and Wnt) between an on and off state or remaining high when on the upper branch? Oscillations in FGF might also trigger a transition to the lower branch (low FGF, high RA) in the bistability domain, with the consequence that oscillations would stop and differentiation would ensue.

## Acknowledgments

We wish to dedicate this article to the memory of Reinhart Heinrich, who made key theoretical contributions to metabolic control analysis, the evolution and optimization of metabolic pathways, and the modeling of biochemical oscillations. His seminal research activities made him a pioneer of Systems Biology. Beyond his many scientific achievements, we will keep the memory of Reinhart's warm personality and radiant smile.

The work of A.G. was supported by Grant #3.4636.04 from the *Fonds de la Recherche Scientifique Médicale* (F.R.S.M., Belgium), by the European Union through the Network of Excellence BioSim, Contract No. LSHB-CT-2004-005137, and by the Belgian Program on Inter-university Attraction Poles, initiated by the Belgian Federal Science Policy Office, Project P6/22 (BioMaGNet). The work of O.P. is supported by the Stowers Institute for Medical Research, NIH Grant R01HD043158, and the DARPA FunBio Program Grant #HR0011-05-1-0057. O.P. is a Howard Hughes Medical Institute Investigator.

## Appendix A. Equations of the model for the Notch, Wnt and FGF oscillators

### A.1. Kinetic equations for oscillations in the Notch signaling module

We incorporate into the model (see Fig. 2c) the activation of the Notch protein by cleavage yielding active Notch in the form of the NICD, the induction of the *Lunatic fringe* gene by NICD, the translation of *Lunatic fringe* mRNA into Lunatic Fringe protein and the negative feedback exerted in a cooperative manner by the Lunatic Fringe protein on the cleavage of Notch into NICD. The variables are the concentrations of the Notch protein ( $N$ ), the cytosolic ( $Na$ ) and nuclear ( $Na_n$ ) forms of the active Notch protein NICD, *Lunatic fringe* mRNA ( $M_F$ ), and Lunatic Fringe protein ( $F$ ). The time evolution of these variables is governed by the following set of kinetic equations:

$$\frac{dN}{dt} = \varepsilon \left[ v_{sN} - v_{dN} \left( \frac{N}{K_{dN} + N} \right) - k_c N \left( \frac{K_{IF}^j}{K_{IF}^j + F^j} \right) \right], \quad (\text{A.1})$$

$$\frac{dNa}{dt} = \varepsilon \left[ k_c N \frac{K_{IF}^j}{K_{IF}^j + F^j} - V_{dNa} \frac{Na}{K_{dNa} + Na} - V_{tr} \right], \quad (\text{A.2})$$

$$\frac{dNa_n}{dt} = \varepsilon \left[ V_{tr} - V_{dNa_n} \frac{Na_n}{K_{dNa_n} + Na_n} \right], \quad (\text{A.3})$$

$$\frac{dM_F}{dt} = \varepsilon \left[ v_{sF} \frac{Na_n^p}{K_A^p + Na_n^p} - v_{mF} \frac{M_F}{K_{dmF} + M_F} \right], \quad (\text{A.4})$$

$$\frac{dF}{dt} = \varepsilon \left[ k_{sF} M_F - v_{dF} \frac{F}{K_{dF} + F} \right] \quad (\text{A.5})$$

with  $V_{tr} = k_{t1}Na - k_{t2}Na_n$ .

The parameters appearing in Eqs. (A.1)–(A.5) are defined in Table A.1, where the parameter values considered for oscillations in the Notch module in Figs. 3 and 4 are listed. Parameter  $\varepsilon$  is a scaling factor that allows us to vary the period of the Notch oscillator relative to the periods of the Wnt and FGF oscillators.

### A.2. Kinetic equations for oscillations in the Wnt signaling module

We consider a simplified scheme for the Wnt signaling pathway (see Fig. 2b) in which  $\beta$ -catenin plays a major

Table A.1

Definitions and values of the parameters used in Figs. 3 and 4 for the model for the segmentation clock based on coupled oscillations in the Notch, Wnt and FGF signaling modules

Parameter	Definition	Numerical value
<i>Notch module</i>		
$v_{sN}$	Maximum rate of Notch synthesis	0.23 nM min <sup>-1</sup>
$v_{dN}$	Maximum rate of Notch degradation	2.82 nM min <sup>-1</sup>
$K_{dN}$	Michaelis constant for Notch degradation	1.4 nM
$k_c$	Apparent first-order rate constant for Notch ( $N$ ) cleavage into NICD ( $Na$ )	3.45 min <sup>-1</sup>
$V_{dNa}$	Maximum rate of NICD degradation	0.01 nM min <sup>-1</sup>
$K_{dNa}$	Michaelis constant for NICD degradation	0.001 nM
$V_{dNa_n}$	Maximum rate of nuclear NICD degradation	0.1 nM min <sup>-1</sup>
$K_{dNa_n}$	Michaelis constant for nuclear NICD degradation	0.001 nM
$K_{IF}$	Threshold constant for inhibition by Lunatic Fringe of Notch cleavage into NICD	0.5 nM
$k_{t1}$	Apparent first-order rate constant for NICD entry into the nucleus	0.1 min <sup>-1</sup>
$k_{t2}$	Apparent first-order rate constant for NICD exit from the nucleus	0.1 min <sup>-1</sup>
$v_{sF}$	Maximum rate of <i>Lunatic fringe</i> gene transcription	3 nM min <sup>-1</sup>
$K_A$	Threshold constant for activation of <i>Lunatic fringe</i> gene transcription by nuclear NICD	0.05 nM
$v_{mF}$	Maximum rate of <i>Lunatic fringe</i> mRNA degradation	1.92 nM min <sup>-1</sup>
$K_{dmF}$	Michaelis constant for <i>Lunatic fringe</i> mRNA degradation	0.768 nM
$k_{sF}$	Apparent first-order rate constant for Lunatic Fringe protein synthesis	0.3 min <sup>-1</sup>
$v_{dF}$	Maximum rate of Lunatic Fringe protein degradation	0.39 nM min <sup>-1</sup>
$K_{dF}$	Michaelis constant for Lunatic Fringe protein degradation	0.37 nM
$K_{IG1}$	Inhibition constant for Gsk inhibition of <i>Lunatic fringe</i> transcription induced by NICD	2.5 nM
$j, p$	Hill coefficients	2
$\varepsilon$	Scaling factor for Notch oscillator	0.3
<i>Wnt module</i>		
$a_1$	Bimolecular rate constant for binding of Gsk3 to Axin2	1.8 nM <sup>-1</sup> min <sup>-1</sup>
$d_1$	Rate constant for dissociation of Gsk3–Axin2 complex	0.1 min <sup>-1</sup>
$v_{sB}$	Maximum rate of $\beta$ -catenin synthesis	0.087 nM min <sup>-1</sup>
$k_{t3}$	Apparent first-order rate constant for $\beta$ -catenin entry into the nucleus	0.7 min <sup>-1</sup>
$k_{t4}$	Apparent first-order rate constant for $\beta$ -catenin exit from the nucleus	1.5 min <sup>-1</sup>
$V_{MK}$	Maximum rate of phosphorylation of $\beta$ -catenin by the kinase Gsk3	5.08 nM min <sup>-1</sup>
$D$	Dishevelled (Dsh) protein concentration	2 nM

Table A.1 (continued)

Parameter	Definition	Numerical value
$K_I$	Total Gsk3 concentration	3 nM
$K_{ID}$	Constant of inhibition by Dishevelled (Dsh) of $\beta$ -catenin phosphorylation by the Axin2–Gsk3 destruction complex	0.5 nM
$K_1$	Michaelis constant for $\beta$ -catenin phosphorylation by the Axin2–Gsk complex	0.28 nM
$V_{MP}$	Maximum rate of dephosphorylation of $\beta$ -catenin	1 nM min <sup>-1</sup>
$K_2$	Michaelis constant for $\beta$ -catenin dephosphorylation	0.03 nM
$k_{d1}$	Apparent first-order rate constant for degradation of unphosphorylated $\beta$ -catenin	0
$k_{d2}$	Apparent first-order rate constant for degradation of phosphorylated $\beta$ -catenin	7.062 min <sup>-1</sup>
$v_0$	Basal rate of transcription of the <i>Axin2</i> gene	0.06 nM min <sup>-1</sup>
$v_{MB}$	Maximum rate of transcription of the <i>Axin2</i> gene induced by nuclear $\beta$ -catenin	1.64 nM min <sup>-1</sup>
$K_{aB}$	Threshold constant for induction by nuclear $\beta$ -catenin of <i>Axin2</i> gene transcription	0.7 nM
$v_{md}$	Maximum rate of degradation of <i>Axin2</i> mRNA	0.8 nM min <sup>-1</sup>
$K_{md}$	Michaelis constant for degradation of <i>Axin2</i> mRNA	0.48 nM
$v_{MXa}$	Maximum rate of transcription of the <i>Axin2</i> gene induced by factor $X_a$	0.5 nM min <sup>-1</sup>
$K_{aXa}$	Threshold constant for induction by factor $X_a$ of <i>Axin2</i> gene transcription	0.05 nM
$k_{sAx}$	Apparent first-order rate constant for synthesis of Axin2 protein	0.02 min <sup>-1</sup>
$v_{dAx}$	Maximum rate of degradation of Axin2 protein	0.6 nM min <sup>-1</sup>
$K_{dAx}$	Michaelis constant for degradation of Axin2 protein	0.63 nM
$n, m$	Hill coefficients	2
$\theta$	Scaling factor for Wnt oscillator	1.5
<i>FGF module</i>		
$Ras_i$	Total concentration of Ras protein	2 nM
$V_{MaRas}$	Maximum rate of activation of Ras	4.968 nM min <sup>-1</sup>
$K_{aFgf}$	Michaelis constant for activation of Ras by FGF	0.5 nM
$Fgf$	FGF concentration	1 nM
$K_{aRas}$	Michaelis constant for activation of Ras by FGF	0.103 nM
$V_{MdRas}$	Maximum rate of inactivation of Ras	0.41 nM min <sup>-1</sup>
$K_{dRas}$	Michaelis constant for inactivation of Ras	0.1 nM
$ERK_i$	Total concentration of ERK protein kinase	2 nM
$V_{MaErk}$	Maximum rate of activation of ERK by Ras	3.30 nM min <sup>-1</sup>
$K_{aErk}$	Michaelis constant for activation of ERK <sub>i</sub>	0.05 nM
$k_{cDusp}$	Catalytic constant of phosphatase Dusp for inactivation of ERK <sub>a</sub>	1.35 min <sup>-1</sup>
$K_{dErk}$	Michaelis constant for inactivation of ERK	0.05 nM
$X_i$	Total concentration of transcription factor X	2 nM
$V_{MaX}$	Maximum rate of activation of X <sub>i</sub> by ERK <sub>a</sub>	1.6 nM min <sup>-1</sup>
$K_{aX}$	Michaelis constant for activation of X <sub>i</sub> by ERK <sub>a</sub>	0.05 nM
$V_{Mdx}$	Maximum rate of inactivation of X <sub>a</sub>	0.5 nM min <sup>-1</sup>
$K_{dX}$	Michaelis constant for inactivation of X <sub>a</sub>	0.05 nM
$V_{MsMDusp}$	Maximum rate of transcription of <i>Dusp6</i> gene induced by transcription factor X	0.9 nM min <sup>-1</sup>
$K_{aMDusp}$	Threshold constant for induction by factor X of <i>Dusp6</i> transcription	0.5 nM
$V_{MdMDusp}$	Maximum rate of degradation of <i>Dusp6</i> mRNA	0.5 nM min <sup>-1</sup>
$K_{dMDusp}$	Michaelis constant for degradation of <i>Dusp6</i> mRNA	0.5 nM
$k_{sDusp}$	Apparent first-order rate constant for synthesis of Dusp6 protein	0.5 min <sup>-1</sup>
$V_{dDusp}$	Maximum rate of degradation of Dusp6 protein	2 nM min <sup>-1</sup>
$K_{dDusp}$	Michaelis constant for degradation of Dusp6 protein	0.5 nM
$q, r$	Hill coefficient	2
$\eta$	Scaling factor for FGF oscillator	0.3

For these parameter values, chosen in a semi-arbitrary manner, the numerical integration of Eqs. (A.1)–(A.16) shows that in the absence of coupling the mRNAs of *Axin2*, *Lunatic fringe* and *MKP3/Dusp6* oscillate with a period close to 66, 113 and 100 min, respectively, while the three modules oscillate synchronously with a period close to 100 min when coupled as described in Eqs. (A.17) and (A.18). Initial conditions are (in nM):  $N=0.5$ ,  $Na=0.2$ ,  $Na_n=0$ ,  $M_F=0.1$ ,  $F=0.01$ ,  $Ras_a=0.5$ ,  $ERK_a=0.2$ ,  $X_a=0.1$ ,  $M_{Dusp}=0.1$ ,  $Dusp=0.1$ ,  $A=0.1$ ,  $K=3$ ,  $B=0.1$ ,  $B_p=0.1$ ,  $B_N=0.001$ ,  $M_{Ax}=0.1$ .

role. This transcription factor triggers the expression of various genes, including the *Axin2* gene. Activation of  $\beta$ -catenin occurs through inhibition of  $\beta$ -catenin degradation. Wnt signaling enhances  $\beta$ -catenin levels by triggering the synthesis of the Dishevelled (Dsh) protein, the level of which will be considered as a parameter measuring the degree of the Wnt pathway stimulation. Dsh acts by inhibiting the kinase Gsk3, which binds to the protein Axin2 to form the destruction complex that promotes

$\beta$ -catenin phosphorylation leading to degradation of the protein. The fact that  $\beta$ -catenin promotes Axin2 synthesis produces a negative feedback loop, because Axin2 participates in the formation of the destruction complex involved in  $\beta$ -catenin degradation.

The variables here are the concentrations of the Axin2 protein ( $A$ ) and *Axin2* mRNA ( $M_{Ax}$ ), the cytosolic forms of nonphosphorylated ( $B$ ) and phosphorylated ( $B_p$ )  $\beta$ -catenin, the nuclear  $\beta$ -catenin ( $B_N$ ), the free kinase

Gsk3 ( $K$ ), and the destruction complex formed between Axin2 and Gsk3 ( $AK$ ). The time evolution of these variables is governed by the following set of kinetic equations:

$$\frac{dK}{dt} = \theta V_1, \quad (\text{A.6})$$

$$\frac{dB}{dt} = \theta \left[ v_{sB} - V_K \frac{AK}{K_t} + V_P + V_2 - k_{d1} B \right], \quad (\text{A.7})$$

$$\frac{dB_p}{dt} = \theta \left[ V_K \frac{AK}{K_t} - V_P - k_{d2} B_p \right], \quad (\text{A.8})$$

$$\frac{dB_N}{dt} = -\theta V_2, \quad (\text{A.9})$$

$$\frac{dM_{Ax}}{dt} = \theta \left[ v_0 + v_{MB} \frac{B_N^n}{K_{aB}^n + B_N^n} - v_{md} \frac{M_{Ax}}{K_{md} + M_{Ax}} \right], \quad (\text{A.10})$$

$$\frac{dA}{dt} = \theta \left[ k_{sAx} M_{Ax} - v_{dAx} \frac{A}{K_{dAx} + A} + V_1 \right] \quad (\text{A.11})$$

with

$$AK = K_t - K,$$

$$V_1 = -a_1 A \cdot K + d_1(AK),$$

$$V_2 = -k_{t3} B + k_{t4} B_N,$$

$$V_K = V_{MK} \left( \frac{K_{ID}}{K_{ID} + D} \right) \left( \frac{B}{K_1 + B} \right),$$

$$V_P = V_{MP} \left( \frac{B_p}{K_2 + B_p} \right).$$

The parameters appearing in Eqs. (A.6)–(A.11) are defined in Table A.1, where the parameter values considered for oscillations in the Wnt module in Figs. 3 and 4 are listed. Parameter  $\theta$  is a scaling factor that allows us to vary the period of the Wnt oscillator relative to the periods of the Notch and FGF oscillators.

### A.3. Kinetic equations for oscillations in the FGF signaling module

We consider a simplified scheme for the FGF signaling pathway (see Fig. 2a) in which FGF binding to its receptor activates, through reversible phosphorylation, the inactive form  $Ras_i$  of the Ras protein into the active form  $Ras_a$ . We describe in a single step the activation by Ras of the MAP kinase cascade that leads to the activation, through reversible phosphorylation, of the protein kinase ERK. The latter kinase activates, through reversible phosphorylation, the inactive form  $X_i$  of a transcription factor X into the active form  $X_a$ . This transcription factor, which likely belongs to the ETS family (Lunn et al., 2007), triggers the expression of the gene *MKP3/Dusp6*, which encodes a protein phosphatase. Based on experimental

evidence that MKP3/Dusp6 is involved in a negative feedback loop (Li et al., 2007), we assume that it counteracts the effect of FGF by inactivating  $ERK_a$  into  $ERK_i$  through dephosphorylation. This negative feedback regulation results in the oscillatory activity of kinase  $ERK_a$  and of transcription factor  $X_a$ , leading to the periodic expression of the gene *MKP3/Dusp6*.

The time evolution of the FGF module is governed by the following kinetic equations Eqs. (A.12)–(A.16) for the concentrations of active Ras ( $Ras_a$ ) and ERK ( $ERK_a$ ), active transcription factor X ( $X_a$ ), *MKP3/Dusp6* mRNA ( $M_{Dusp}$ ), and MKP3/Dusp6 protein ( $Dusp$ ):

$$\frac{dRas_a}{dt} = \eta(V_{aRas} - V_{dRas}), \quad (\text{A.12})$$

$$\frac{dERK_a}{dt} = \eta(V_{aErk} - V_{dErk}), \quad (\text{A.13})$$

$$\frac{dX_a}{dt} = \eta(V_{aX} - V_{dX}), \quad (\text{A.14})$$

$$\frac{dM_{Dusp}}{dt} = \eta(V_{sM_{Dusp}} - V_{dM_{Dusp}}), \quad (\text{A.15})$$

$$\frac{dDusp}{dt} = \eta \left[ k_{sDusp} M_{Dusp} - V_{dDusp} \left( \frac{Dusp}{K_{dDusp} + Dusp} \right) \right] \quad (\text{A.16})$$

with

$$Ras_i = Ras_t - Ras_a,$$

$$V_{aRas} = V_{MaRas} \left( \frac{Fgf^r}{K_{aFgf}^r + Fgf^r} \right) \left( \frac{Ras_i}{K_{aRas} + Ras_i} \right),$$

$$V_{dRas} = V_{MdRas} \left( \frac{Ras_a}{K_{dRas} + Ras_a} \right),$$

$$ERK_i = ERK_t - ERK_a,$$

$$V_{aErk} = V_{MaErk} \left( \frac{Ras_a}{Ras_t} \right) \left( \frac{ERK_i}{K_{aErk} + ERK_i} \right),$$

$$V_{dErk} = k_{cDusp} Dusp \left( \frac{ERK_a}{K_{dErk} + ERK_a} \right),$$

$$X_a = X_t - X_i,$$

$$V_{aX} = V_{MaX} \left( \frac{ERK_a}{ERK_t} \right) \left( \frac{X_i}{K_{aX} + X_i} \right),$$

$$V_{dX} = V_{MdX} \left( \frac{X_a}{K_{dX} + X_a} \right),$$

$$V_{sM_{Dusp}} = V_{MsM_{Dusp}} \left( \frac{X_a^q}{K_{aM_{Dusp}}^q + X_a^q} \right),$$

$$V_{dMDusp} = V_{MdMDusp} \left( \frac{M_{Dusp}}{K_{dMDusp} + M_{Dusp}} \right).$$

The parameters appearing in Eqs. (A.12)–(A.16) are defined in Table A.1, where the parameter values considered for oscillations in the FGF module in Figs. 3 and 4 are listed. The scaling factor  $\eta$  allows us to vary the period of the FGF oscillator relative to the periods of the Wnt and Notch oscillators.

#### A.4. Kinetic equations for oscillations in the coupled Notch, FGF and Wnt signaling modules

The coupled system is governed by Eqs. (A.1)–(A.16), with the following changes described in Eqs. (A.17) and (A.18) below:

- (1) The maximum rate  $v_{sF}$  of expression of the *Lunatic fringe* gene in Eq. (A.4) is replaced by  $v_{sFK}$  given by the following expression:

$$v_{sFK} = v_{sF} \left( \frac{K_{IG1}}{K_{IG1} + K} \right). \quad (\text{A.17})$$

Equation Eq. (A.17) expresses the putative inhibition exerted by the free form of the kinase Gsk3 ( $K$ ) on the expression of the *Lunatic fringe* gene. The time evolution of  $K$  in the Wnt pathway is given by Eq. (A.6).

- (2) Eq. (A.10) must be replaced by Eq. (A.18):

$$\frac{dM_{Ax}}{dt} = \theta \left[ v_0 + v_{MB} \frac{B_N^n}{K_{aB}^n + B_N^n} + v_{MXa} \frac{X_a^m}{K_{aXa}^m + X_a^m} - v_{md} \frac{M_{Ax}}{K_{md} + M_{Ax}} \right] \quad (\text{A.18})$$

which expresses the hypothesis that the transcription of the gene *Axin2* is induced not only by  $\beta$ -catenin activated in the Wnt pathway but also by transcription factor X activated in the FGF pathway.

The new parameters appearing in Eqs. (A.17) and (A.18) are listed in Table A.1, together with their values used in Fig. 4.

## References

Aulehla, A., Wehrle, C., Brand-Saberi, B., Kemler, R., Gossler, A., Kanzler, B., Herrmann, B.G., 2003. Wnt3a plays a major role in the segmentation clock controlling somitogenesis. *Dev. Cell* 4, 395–406.

Bessho, Y., Hirata, H., Masamizu, Y., Kageyama, R., 2003. Periodic repression by the bHLH factor Hes7 is an essential mechanism for the somite segmentation clock. *Genes Dev.* 17, 1451–1456.

Cooke, J., Zeeman, E.C., 1976. A clock and wavefront model for control of the number of repeated structures during animal morphogenesis. *J. Theor. Biol.* 58, 455–476.

Dale, J.K., Maroto, M., Dequeant, M.L., Malapert, P., McGrew, M., Pourquie, O., 2003. Periodic notch inhibition by lunatic fringe underlies the chick segmentation clock. *Nature* 421, 275–278.

Delfini, M.C., Dubrulle, J., Malapert, P., Chal, J., Pourquie, O., 2005. Control of the segmentation process by graded MAPK/ERK activation in the chick embryo. *Proc. Natl. Acad. Sci. U.S.A.* 102, 11343–11348.

Dequeant, M.L., Glynn, E., Gaudenz, K., Wahl, M., Chen, J., Mushegian, A., Pourquie, O., 2006. A complex oscillating network of signaling genes underlies the mouse segmentation clock. *Science* 314, 1595–1598.

Dubrulle, J., Pourquie, O., 2004. FGF8 mRNA decay establishes a gradient that couples axial elongation to patterning in the vertebrate embryo. *Nature* 427, 419–422.

Dunlap, J.C., 1999. Molecular bases for circadian clocks. *Cell* 96, 271–290.

Espinosa, L., Ingles-Esteve, J., Aguilera, C., Bigas, A., 2003. Phosphorylation by glycogen synthase kinase-3 beta down-regulates Notch activity, a link for Notch and Wnt pathways. *J. Biol. Chem.* 278, 32227–32235.

Galceran, J., Sustmann, C., Hsu, S.C., Folberth, S., Grosschedl, R., 2004. LEF1-mediated regulation of Delta-like1 links Wnt and Notch signaling in somitogenesis. *Genes Dev.* 18, 2718–2723.

Giudicelli, F., Lewis, J., 2004. The vertebrate segmentation clock. *Curr. Opin. Genet. Dev.* 14, 407–414.

Goldbeter, A., 1996. *Biochemical Oscillations and Cellular Rhythms. The Molecular Bases of Periodic and Chaotic Behaviour.* Cambridge Univ. Press, Cambridge, UK.

Goldbeter, A., 2002. Computational approaches to cellular rhythms. *Nature* 420, 238–245.

Goldbeter, A., Gonze, D., Pourquie, O., 2007. Sharp developmental thresholds defined through bistability by antagonistic gradients of retinoic acid and FGF signaling. *Dev. Dyn.* 236, 1495–1508.

Hirata, H., Yoshiura, S., Ohtsuka, T., Bessho, Y., Harada, T., Yoshikawa, K., Kageyama, R., 2002. Oscillatory expression of the bHLH factor Hes1 regulated by a negative feedback loop. *Science* 298, 840–843.

Hirata, H., Bessho, Y., Kokubu, H., Masamizu, Y., Yamada, S., Lewis, J., Kageyama, R., 2004. Instability of Hes7 protein is crucial for the somite segmentation clock. *Nat. Genet.* 36, 750–754.

Hofmann, M., Schuster-Gossler, K., Watabe-Rudolph, M., Aulehla, A., Herrmann, B.G., Gossler, A., 2004. WNT signaling, in synergy with T/TBX6, controls Notch signaling by regulating Dll1 expression in the presomitic mesoderm of mouse embryos. *Genes Dev.* 18, 2712–2717.

Ishikawa, A., Kitajima, S., Takahashi, Y., Kokubo, H., Kanno, J., Inoue, T., Saga, Y., 2004. Mouse Nkd1, a Wnt antagonist, exhibits oscillatory gene expression in the PSM under the control of Notch signaling. *Mech. Dev.* 121, 1443–1453.

Jiang, Y.J., Aerne, B.L., Smithers, L., Haddon, C., Ish-Horowicz, D., Lewis, J., 2000. Notch signalling and the synchronization of the somite segmentation clock. *Nature* 408, 475–479.

Katoh, Y., Katoh, M., 2006. FGF signaling inhibitor, SPRY4, is evolutionarily conserved target of WNT signaling pathway in progenitor cells. *Int. J. Mol. Med.* 17, 529–532.

Kim, Y., Kobayashi, A., Sekido, R., DiNapoli, L., Brennan, J., Chaboissier, M.C., Poulat, F., Behringer, R.R., Lovell-Badge, R., Capel, B., 2006. Fgf9 and Wnt4 act as antagonistic signals to regulate mammalian sex determination. *PLoS Biol.* 4, 1000–1009.

Krüger, R., Heinrich, R., 2004. Model reduction and analysis of robustness for the Wnt/beta-catenin signal transduction pathway. *Genome Inform.* 15, 138–148.

Lee, E., Salic, A., Krüger, R., Heinrich, R., Kirschner, M.W., 2003. The roles of APC and Axin derived from experimental and theoretical analysis of the Wnt pathway. *PLoS Biol.* 1, 116–132.

Lewis, J., 2003. Autoinhibition with transcriptional delay: a simple mechanism for the zebrafish somitogenesis oscillator. *Curr. Biol.* 13, 1398–1408.

Li, C., Scott, D.A., Hatch, E., Tian, X., Mansour, S.L., 2007. Dusp6 (Mkp3) is a negative feedback regulator of FGF-stimulated ERK signaling during mouse development. *Development* 134, 167–176.

Lunn, J.S., Fishwick, K.J., Halley, P.A., Storey, K.G., 2007. A spatial and temporal map of FGF/Erk1/2 activity and response repertoires in the early chick embryo. *Dev. Biol.* 302, 536–552.

- Monk, N.A., 2003. Oscillatory expression of Hes1, p53, and NF-kappaB driven by transcriptional time delays. *Curr. Biol.* 13, 1409–1413.
- Morimoto, M., Takahashi, Y., Endo, M., Saga, Y., 2005. The Mesp2 transcription factor establishes segmental borders by suppressing Notch activity. *Nature* 435, 354–359.
- Niwa, Y., Masamizu, Y., Liu, T., Nakayama, R., Deng, C.X., Kageyama, R., 2007. The initiation and propagation of Hes7 oscillation are cooperatively regulated by Fgf and notch signaling in the somite segmentation clock. *Dev. Cell* 13, 298–304.
- Olivera-Martinez, I., Storey, K.G., 2007. Wnt signals provide a timing mechanism for the FGF-retinoid differentiation switch during vertebrate body axis extension. *Development* 134, 2125–2135.
- Palmeirim, I., Henrique, D., Ish-Horowicz, D., Pourquie, O., 1997. Avian hairy gene expression identifies a molecular clock linked to vertebrate segmentation and somitogenesis. *Cell* 91, 639–648.
- Pourquie, O., 2003. The segmentation clock: converting embryonic time into spatial pattern. *Science* 301, 328–330.
- Riedel-Kruse, I.H., Müller, C., Oates, A.C., 2007. Synchrony dynamics during initiation, failure, and rescue of the segmentation clock. *Science* 317, 1911–1915.
- Rodriguez-Gonzalez, J.G., Santillan, M., Fowler, A.C., Mackey, M.C., 2007. The segmentation clock in mice: Interaction between the Wnt and Notch signalling pathways. *J. Theor. Biol.* 248, 37–47.
- Serth, K., Schuster-Gossler, K., Cordes, R., Gossler, A., 2003. Transcriptional oscillation of lunatic fringe is essential for somitogenesis. *Genes Dev.* 17, 912–925.
- Wahl, M.B., Deng, C., Lewandoski, M., Pourquie, O., 2007. FGF signaling acts upstream of the NOTCH and WNT signaling pathways to control segmentation clock oscillations in mouse somitogenesis. *Development* 134, 4033–4041.